Int J Clin Exp Med 2018;11(3):1669-1678
www.ijcem.com /ISSN:1940-5901/IJCEM0062792

Original Article

Bioinformatic analysis of gene expression profile in prostate epithelial cells exposed to low-dose cadmium

Qiling Liu[1,2*], Rongqiang Zhang[2*], Xiang Wang[1], Peili Wang[2], Xiaomei Ren[2], Na Sun[2], Xiangwen Li[2], Xinhui Li[2], Chunxu Hai[1]

[1]Department of Toxicology, The Ministry of Education Key Lab of Hazard Assessment and Control in Special Operational Environment, Shaanxi Provincial Key Lab of Free Radical Biology and Medicine, School of Public Health, Medical University of The Air Force, Xi'an, Shaanxi 710032, China; [2]Department of Epidemic and Health Statistics, The College of Public Health for The Shaanxi University of Chinese Medicine, Shaanxi 712046, China. [*]Equal contributors.

Received July 25, 2017; Accepted February 5, 2018; Epub March 15, 2018; Published March 30, 2018

Abstract: Objective: This study was to identify key genes and biological pathways involved in responses of prostate epithelial cells after low-dose Cd exposure by using bioinformatic analysis. Methods: The gene chip data of prostate epithelial cells after low-dose Cd exposure were collected from public databases Gene Expression Omnibus. After identification of differentially expressed genes (DEGs), data were input into Qlucore Omics Explorer, Network Analyst, String, and Genclip for further analysis of gene expression profiles, protein-protein interactions (PPI) and protein-chemicals interactions, and critical molecular pathways. Results: A total of 384 DEGs were identified in Cd treated group compared with control group. The number of DEGs gradually decreased over time, with the largest number at 0 h. Furthermore, NDUFB5 (A, S), CYC1, UQCRB, ETFA (B), SNRPD2, and LSM3 (5, 6) were the hub proteins in the PPI network. A functionally grouped DEGs network was established, and the oxidative phosphorylation and mitochondrial ATP synthesis coupled electron transport signaling pathways were significantly enriched. Main genes related to Cd treatment were CYP1B1, STAT1, RPS27L, FKBP5, TYMS, and IDH1. Conclusions: Our results show that oxidative phosphorylation, especially mitochondrial oxidative phosphorylation significantly related to NAD[P]H, represents the main mechanism of NPrEC damage after low-dose Cd exposure. Low-dose Cd induces transient over-expression of relevant genes and causes the release of NAD[P]H from its normal protein binding sites, resulting in a disruption of the enzyme and protein activities and leading to subsequent toxic events.

Keywords: Cadmium, bioinformatic analysis, gene expression profile, prostate epithelial cells

Introduction

Prostate cancer has high morbidity and mortality in male adults. It has been the most common cancer and the second leading cause of cancer-related death in American men [1]. In China, the incidence of prostate cancer is lower than Western countries, but a rising trend is shown in recent years [2]. In spite of great advance achieved on molecular mechanisms involved in pathogenesis of prostate cancer, particularly role of androgen signaling [3], further efforts are still needed to clearly elucidate complex etiology of this disease, especially roles of genetic background, age, physiological status, lifestyle, and environmental risk factors [4].

Cadmium (Cd), an environmental and industrial pollutant, is released into the environment through the waste from heavy metal mining, manufacture of nickel-cadmium batteries, and other industrial and agricultural activities [5]. It can be easily absorbed by plants and animals, and eventually accumulate in human via the food chain, thus causing injuries [6]. Cd and Cd compounds have been classified by the International Agency for Research on Cancer and the U. S. National Toxicology Program as Group 1 human carcinogen. Non-occupational exposure to Cd is mainly from diet and smoking [7]. The targets of Cd include liver, lung, kidney cortex, bone, cardiovascular system, and immune system [8]. Recently, it has been demonstrated that Cd can cause prostate injuries

Table 1. The top 50 differentially expressed genes identified in low-dose Cd treated NPrEC cells versus control cells

NO.	Gene name	Abbreviation	NO.	Gene name	Abbreviation
1	Archaelysin family metallopeptidase 2	AMZ2	26	F-box protein 22	FBXO22
2	isocitrate dehydrogenase (NADP(+)) 1, cytosolic	IDH1	27	deoxyribose-phosphate aldolase	DERA
3	ADP ribosylation factor like GTPase 6 interacting protein 5	ARL6IP5	28	COMM domain containing 10	COMMD10
4	thymidylate synthetase	TYMS	29	synaptophysin like 1	SYPL1
5	NADH:ubiquinone oxidoreductase subunit B5	NDUFB5	30	growth arrest specific 1	GAS1
6	F-box protein 4	FBXO4	31	general transcription factor IIH subunit 5	GTF2H5
7	FK506 binding protein 5	FKBP5	32	heterogeneous nuclear ribonucleoprotein F	HNRNPF
8	ubiquinol-cytochrome c reductase core protein II	UQCRC2	33	OCIA domain containing 1	OCIAD1
9	tripartite motif containing 14	TRIM14	34	signal transducer and activator of transcription 1	STAT1
10	alcohol dehydrogenase 5 (class III), chi polypeptide	ADH5	35	LSM3 homolog, U6 small nuclear RNA and mRNA degradation associated	LSM3
11	cytochrome P450 family 1 subfamily B member 1	CYP1B1	36	nicotinamide riboside kinase 1	NMRK1
12	transmembrane protein 19	TMEM19	37	churchill domain containing 1	CHURC1
13	electron transfer flavoprotein alpha subunit	ETFA	38	tetraspanin 6	TSPAN6
14	cereblon	CRBN	39	ADP ribosylation factor like GTPase 6 interacting protein 5	ARL6IP5
15	ubiquinol-cytochrome c reductase binding protein	UQCRB	40	translocase of inner mitochondrial membrane 23 homolog B///translocase of inner mitochondrial membrane 23	TIMM23B/// TIMM23
16	serine racemase	SRR	41	phosphatidylinositol glycan anchor biosynthesis class F	PIGF
17	glucosamine-6-phosphate deaminase 1	GNPDA1	42	acireductone dioxygenase 1	ADI1
18	CD1d molecule	CD1D	43	GLI family zinc finger 3	GLI3
19	collagen type VIII alpha 1 chain	COL8A1	44	H3 histone, family 3A, pseudogene 4///H3 histone, family 3B///H3 histone, family 3A	H3F3AP4/// H3F3B///H3F3A
20	serine racemase	SRR	45	pyrophosphatase (inorganic) 2	PPA2
21	H3 histone, family 3A, pseudogene 4///H3 histone, family 3B///H3 histone, family 3A	H3F3AP4/// H3F3B///H3F3A	46	general transcription factor IIA subunit 2	GTF2A2
22	lysosomal protein transmembrane 4 beta	LAPTM4B	47	transcription factor like 5	TCFL5
23	translocase of outer mitochondrial membrane 22	TOMM22	48	progesterone receptor membrane component 1	PGRMC1
24	transmembrane protein 230	TMEM230	49	ribosomal protein S27 like	RPS27L
25	lysosomal protein transmembrane 4 beta	LAPTM4B	50	cytochrome c oxidase copper chaperone	COX11

[9]. For years, different possible mechanisms have been proposed for the Cd related carcinogenesis [8, 10, 11], but molecular pathways involved in this process are still unclear. Several mechanisms have been proposed, including the generation of reactive oxygen species (ROS) and nitric oxide synthase responsible for oxidative and nitrosative stress [12-15], the activation of proto-oncogenes, the alteration of DNA methylation, the dysregulation of gene expression [16], and other processes.

In this study, the public microarray dataset GSE9951 constructed by Bakshi et al [17] was analyzed, and the differentially expressed genes were identified in the prostate epithelial cell line NPrEC exposed to low-dose Cd. Gene ontology (GO) and pathway enrichment analyses were performed to identify the up- and down-regulated genes. Furthermore, the PPI and PCI regulating DEGs were predicted, and the key regulatory network was built. Our results may contribute to a better understanding of the molecular oncogenesis of prostate diseases caused by low-dose Cd exposure.

Materials and methods

Affymetrix microarray data

The gene expression data GSE9951 were downloaded from the public database Gene Expression Omnibus (GEO, http://www.ncbi.nlm.nih.gov/geo/) by using the platform [HG-U133_Plus_2] Affymetrix Human Genome U133 Plus 2 Array (GPL570, Affymetrix Inc, Cincinnati, OH,

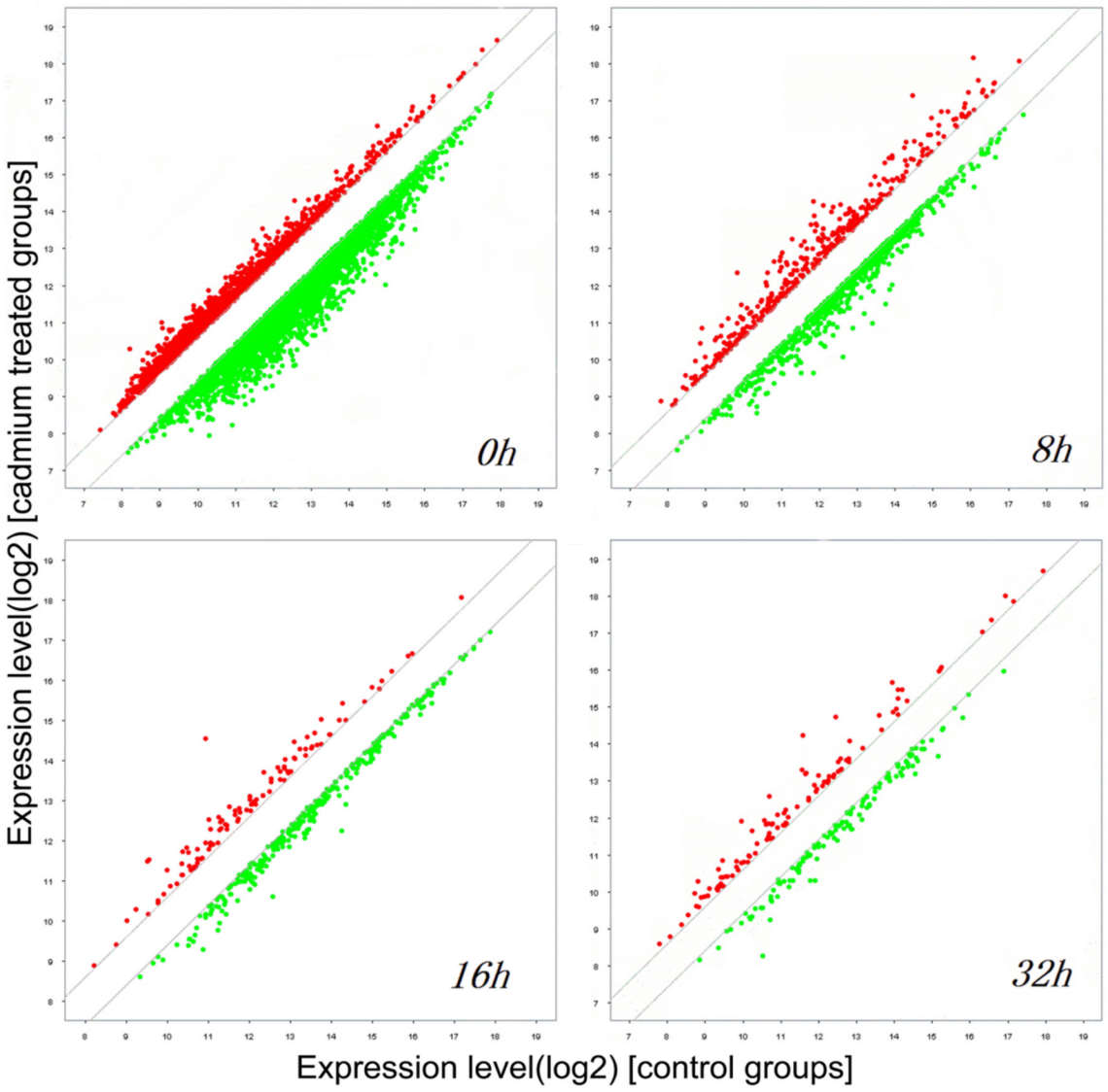

Figure 1. Gene expression profile at different time points. Red dots: up-regulated DEGs; green dots: down-regulated DEGs.

USA). This dataset contained 19 samples with each experimental condition having two biological replicates, except one sample in cadmium 4 h. Cd-treated and control samples were collected at 0, 4, 8, 16, and 32 h.

DEGs screening

The CEL raw data were downloaded and preprocessed by using the package oligo for Bioconductor (http://www.bioconductor.org/packages/release/bioc/html/) in R environment. The method of robust multiarray average was used. The preprocessing process included background correction, quartile data normalization and probe summarization. The false discovery rate was calculated to adjust the *P*-value with Benjamini-Hochberg method. Only genes meeting |log2FC| ≥0.50 and an adjusted *P*-value <0.05 were considered as DEGs.

Expression profile analysis

Preprocessed dataset GSE9951 was imported into Qlucore Omics Explorer 3.1 software, standardized (Mean=0, SD=1), filtered, and analyzed with t-test ($p<0.01$, $q<0.01$). Finally, the data were clustered with Principal Components Analysis (PCA) and Hierarchical cluster analysis.

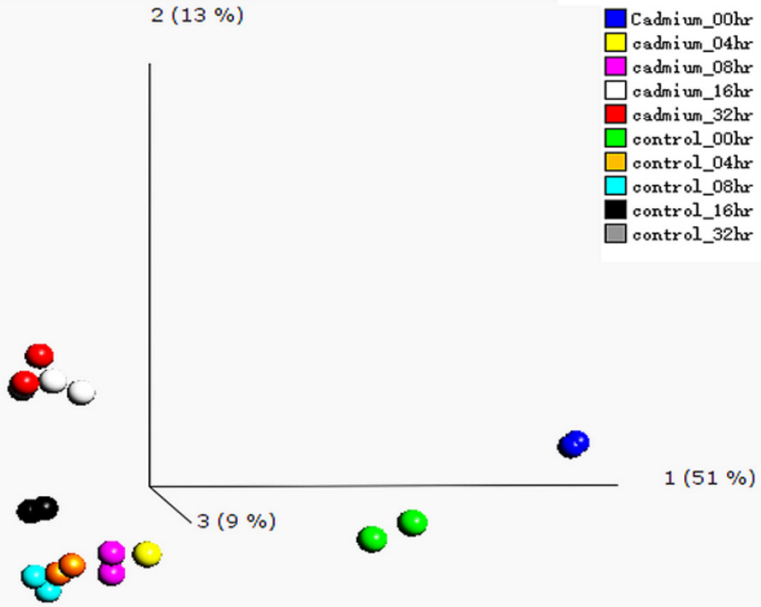

Figure 2. Principal component analysis of differentially expressed genes between Cd treated cells and control cells.

PPI network construction

A PPI network of DEGs was constructed by using Search Tool for the Retrieval of Interacting Genes/Proteins database, with the threshold combined score of >0.4. In the PPI network, nodes and edges (lines) represent proteins and their interactions, respectively. Nodes with an average node connective degree ≥9 were considered as hub proteins.

Enrichment analysis for DEGs

The Database for Annotation, Visualization and Integrated Discovery (https://david.ncifcrf.gov/), which uses analytical tools to extract biological functions for numerous genes, was used for enrichment analysis. The top 50 DEGs were independently input into the human gene function and network analysis software GenClip2.0 for GO and Kyoto Encyclopedia of Genes and Genomes (KEGG) functional and pathway enrichment analysis. The *p*-value <0.05 and gene count ≥2 were used as cut-off criteria. The primary parameters were adjusted if needed.

Results

Identification of DEGs

GSE9951 database contained 54675 genes. Based on the cut-off criteria, a total of 384 genes were identified as differentially expressed gene between two analyzed groups. The top 50 DEGs are shown in **Table 1**.

Gene expression profiling

The gene expression profiles were detected at 4 time points: 0 h, 8 h, 16 h and 32 h. Results showed that there were 4348 differentially expressed genes at 0 h including 1498 with up-regulated expression and 2850 with down-regulated expression; there were 1138 DEGs at 8 h, including 380 up-regulated and 758 down-regulated genes; there were only 399 DEGs at 16 h, including 104 up-regulated and 295 down-regulated genes; at 32 h there were 240 DEGs, including 108 up-regulated and 132 down-regulated genes (**Figure 1**). This suggests that the number of differentially expressed genes in the Cd exposed prostate epithelial cells decreased over time, and continuous Cd exposure reduces gene expression.

According to the gene expression pattern, the principal component analysis (PCA) was performed for these genes. As shown in **Figure 2**, X, Y, and Z axis data variance contribution rates were 9%, 51% and 13%, respectively. Only samples at 0 h clustered on the Y axis, suggesting that the most significant differences between Cd treated cells and control cells were present at 0 h.

PPI network construction

The obtained PPI network based on the top 50 DEGs between two groups is reported in **Figure 3**. The top hub proteins were NDUFB5 (A, S), CYC1, UQCRB, ETFA (B), SNRPD2, and LSM3 (5, 6). Interestingly, all these key proteins are related to mitochondrial redox.

GO functional enrichment analysis of DEGs

The top 50 DEGs in two groups were inspected for enriched GO terms related to oxidative phosphorylation and mitochondrial ATP synthesis coupled electron transport (**Table 2**).

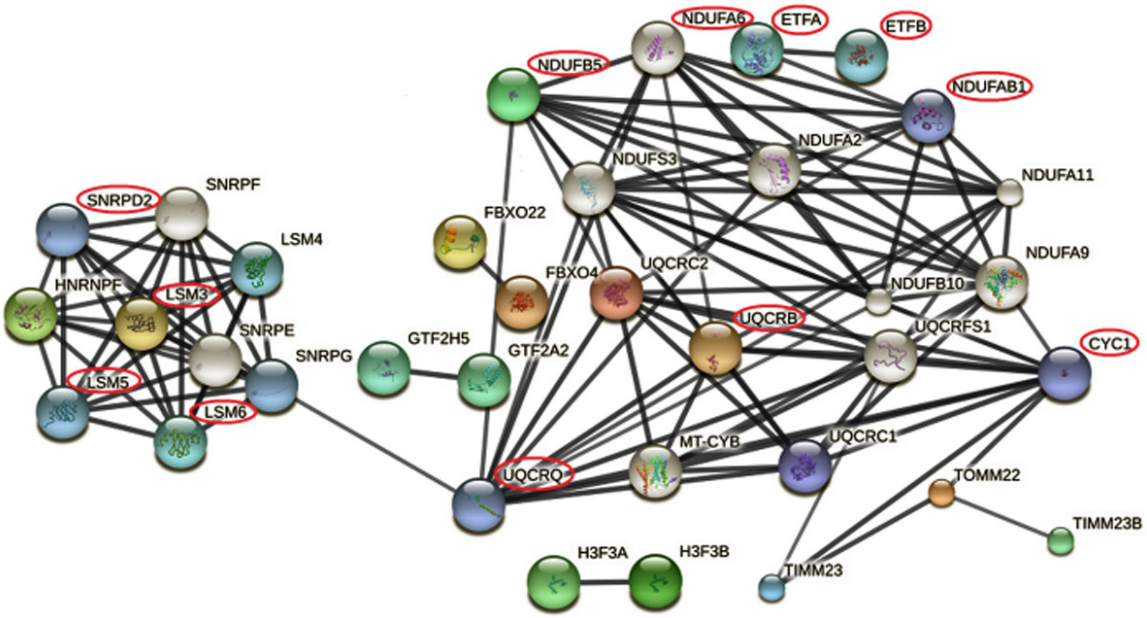

Figure 3. The obtained PPI network for the top 50 DEGs.

Table 2. Functional enrichment analysis of top 50 DEGs of Cd treated cells and control cells

	Term	Number	*P*-value
BP	GO:0006119-oxidative phosphorylation	17	1.81E-09
	GO:0022904-respiratory electron transport chain	10	4.75E-16
	GO:0006091-generation of precursor metabolites and energy	9	1.09E-11
	GO:0042775-mitochondrial ATP synthesis coupled electron transport	15	1.1E-11
CC	GO:0098798-mitochondrial protein complex	16	5.74E-19
	GO:0098800-inner mitochondrial membrane protein complex	15	5.74E-19
	GO:0098803-respiratory chain complex	13	9.12E-18
	GO:1990204-oxidoreductase complex	13	1.01E-15
MF	GO:0008137-NADH dehydrogenase (ubiquinone) activity	7	2.32E-07
	GO:0016491-oxidoreductase activity	16	2.32E-07
	GO:0008121-ubiquinol-cytochrome-c reductase activity	4	4.28E-06
	GO:0009055-electron carrier activity	6	0.000336
	GO:0008320-protein transmembrane transporter activity	3	0.00826
KEGG	00190-Oxidative phosphorylation	15	3.64E-17
	05012-Parkinson s disease	14	2.37E-15
	04932-Non-alcoholic fatty liver disease (NAFLD)	14	3.52E-15

Note: BP: Biological Process; CC: Cellular Component; MF: Molecular Function; KEGG: Kyoto Encyclopedia of Genes and Genomes.

GO functional enrichment diagram of DEGs

Genclip online software was used to obtain the GO functional enrichment diagram for the top 50 DEGs. As reported in **Figure 4**, highly expressed genes included ATP5G3, NDUFB5, UQCRC2, TYMS, MGST1 and COX11, in good agreement with previous results.

KEGG enrichment analysis of DEGs

The top 50 DEGs were significantly enriched in three signaling pathways: oxidative phosphorylation (NDUFB5, ETFA), electron transport chain (NDUFB5, UQCRB, ATP5G3) and glucose regulation of insulin secretion (UQCRB, UQCRC2, ATP5G3) (**Figure 5**).

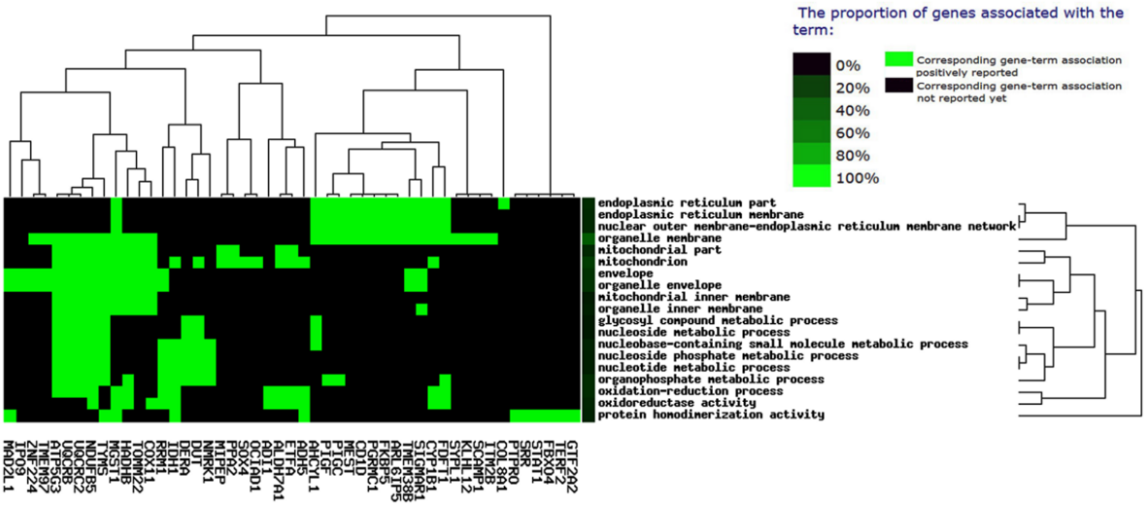

Figure 4. Histogram of enriched Go terms of the top 50 DEGs.

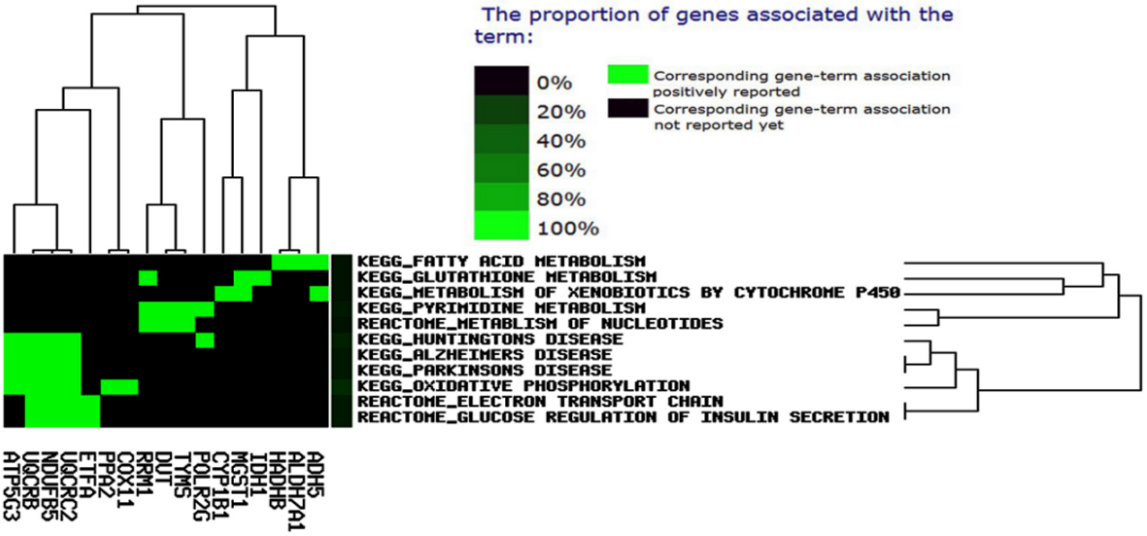

Figure 5. Histogram of KEGG analysis of DEGs.

Protein-chemicals interactions

As reported in **Figure 6**, the main genes significantly related to Cd treatment were CYP1B1, STAT1, RPS27L, FKBP5, TYMS, and IDH1. All these genes are closely associated with mitochondrial function and play an essential role in the oxidative function.

Discussion

Prostate cancer is highly prevalent in older men and has been a leading cause of cancer related death from in men worldwide. The etiology of prostate cancer is complex and related to a lot of factors including age, race, environmental and lifestyle [18, 19]. Some environmental factors such as Cd exposure are less well studied than the aforementioned factors [20].

Cd has been classified as a human carcinogen by the International Agency for Research on Cancer (IARC, 1993) and the National Toxicology Program (NTP, 2004) [21]. Cd can affect human health mainly through the food chain. Because of its very slow excretion rate (~0.001%/day) [22], Cd accumulates in human over time [23], and the prostate is one of organs with high bioaccumulation of Cd (0.45-28 μM) [24]. Thus, the bioaccumulation and toxic effects of Cd due to the exposure to low-dose Cd have attracted considerable attention.

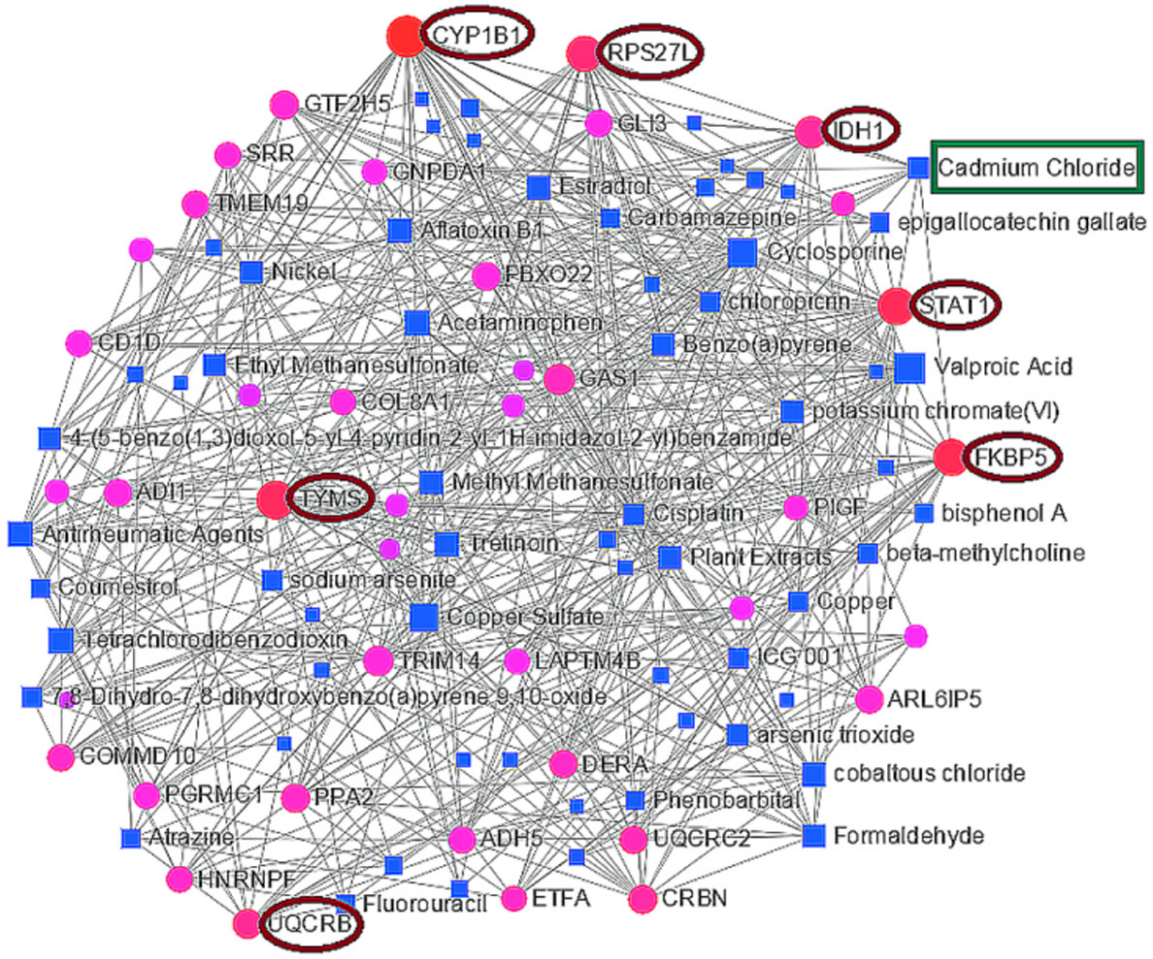

Figure 6. Protein-chemicals interactions. Red and pink dots: DEGs; blue square: key chemicals.

Previous studies have shown that Cd exposure is significantly associated with prostate cancer [25, 26], but the specific mechanisms are still poorly understood. The rapid development of omics-based techniques coupled to bioinformatic analysis can help the elucidation of possible mechanisms related to low-dose Cd exposure in prostate cancer.

In the present study, bioinformatic analysis was performed to investigate the differentially expressed genes after low-dose Cd exposure in NPrEC. The public microarray dataset N. GSE9951 constructed by Bakshi et al was used to identify the key genes and pathways involved in Cd-induced injury. A total of 384 DEGs were identified, and the number of DEGs decreased over time. Indeed, at 0 h, differences in gene expression between Cd treated and control cells were the most significant. We speculate that low-dose Cd exposure induces transient over-expression of genes related to the resistance to Cd toxicity. However, the gene expression decreases over time due to the toxicity of Cd. Some *in-vivo* experiments [5, 27, 28] have demonstrated that Cd rapidly and transiently induces intracellular ROS formation soon after Cd exposure, and then ROS decreased to a level below the baseline after 6 h.

The PPI network constructed on the basis of top 50 DEGs revealed that the hub genes were NDUFB5, CYC1, UQCRB, ETFA, SNRPD, and LSM3. These key genes are all related to mitochondrial redox [29-34]. For example, CYC1 accepts electrons from Rieske protein and then transfers electrons to cytochrome c in the mitochondrial respiratory chain [32]; UQCRB is a part of mitochondrial respiratory chain. It takes part in the oxidation-reduction and may affect the oxidoreductase activity *via* ETF-ubiquinone oxidoreductase [33]. These findings indicate that the mitochondrial oxidative stress is involved in Cd-induced damage. Indeed, Bertin

and Averbeck [35] demonstrated that Cd induced oxidative stress in many organisms, resulting in damages to different organs like the kidney, liver, lung, pancreas, testes, placenta, and bone. We hypothesize that the Cd-induced damage to prostate cells may also be related to the excessive ROS production due to mitochondrial oxidative phosphorylation. The significantly enriched biological processes related to oxidative phosphorylation and mitochondrial ATP synthesis coupled electron transport identified in this study confirmed our hypothesis above. Analysis of signaling pathways also revealed the enrichment of oxidative phosphorylation (NDUFB5, ETFA) and mitochondrial electron transport chain (NDUFB5, UQCRB, ATP5G3).

Finally, the interactions between proteins and chemicals were further analyzed, and results showed that the key proteins related to Cd toxicity were CYP1B1, STAT1, RPS27L, FKBP5, TYMS, and IDH1. CYP1B1 is an enzyme involved in NADPH-dependent electron transport pathway and can oxidize a variety of structurally unrelated compounds, including steroids, fatty acids, and retinoids. RPS27L plays a role in cysteine-type endopeptidase activity involved in apoptosis and metal ion binding [36]. These indicate that these genes are associated with mitochondrial oxidative stress and cell apoptosis. In conclusion, our study suggest that low-dose Cd exposure may cause mitochondrial redox imbalance in prostate epithelial cells, under which the NADPH changes electron transport chain status, leading to the subsequent toxic events, such as cell apoptosis. The novelty of the study include that: we predict the key biomarkers and possible molecular mechanisms of chronic cadmium exposure to prostate damage by genomics and data mining techniques; It is further clarified that the time and quantity effect of chronic cadmium exposure leads to transcription spectrum changes; The key genes of the prostate mitochondria REDOX imbalance was clarified, and this may provide a basis for the study of mitochondrial oxidative damage.

Acknowledgements

This study was supported by the national natural science foundation of China (No. 81473010) and Shaanxi natural science fund (No. 2016JM8031) and Shaanxi Administration of Traditional Chinese Medicine fund (No. JCMS035).

Disclosure of conflict of interest

None.

Address correspondence to: Chunxu Hai, Department of Toxicology, School of Public Health, Medical University of The Air Force, Shaanxi Provincial Key Lab of Free Radical Biology and Medicine, The Ministry of Education Key Lab of Hazard Assessment and Control in Special Operational Environment, Xi'an, Shaanxi 710032, China. Tel: +86-02984772951; Fax: +86-02984772951; E-mail: cxhai@fmmu.edu.cn

References

[1] Gunnarsdottir S, Sigurdardottir V, Kloke M, Radbruch L, Sabatowski R, Kaasa S and Klepstad P. A multicenter study of attitudinal barriers to cancer pain management. Support Care Cancer 2017; 25: 3595-3602.

[2] Tse LA, Lee PMY, Ho WM, Lam AT, Lee MK, Ng SSM, He Y, Leung KS, Hartle JC, Hu H, Kan H, Wang F and Ng CF. Bisphenol A and other environmental risk factors for prostate cancer in Hong Kong. Environ Int 2017; 107: 1-7.

[3] Inoue S, Mizushima T and Miyamoto H. Role of the androgen receptor in urothelial cancer. Mol Cell Endocrinol 2017; [Epub ahead of print].

[4] Srut M, Drechsel V and Hockner M. Low levels of Cd induce persisting epigenetic modifications and acclimation mechanisms in the earthworm Lumbricus terrestris. PLoS One 2017; 12: e0176047.

[5] Anetor JI. Rising environmental cadmium levels in developing countries: threat to genome stability and health. Niger J Physiol Sci 2012; 27: 103-115.

[6] Ye X, Ling T, Xue Y, Xu C, Zhou W, Hu L, Chen J and Shi Z. Thymol mitigates cadmium stress by regulating glutathione levels and reactive oxygen species homeostasis in tobacco seedlings. Molecules 2016; 21.

[7] Yuan Y, Ma S, Qi Y, Wei X, Cai H, Dong L, Lu Y, Zhang Y and Guo Q. Quercetin inhibited cadmium-induced autophagy in the mouse kidney via inhibition of oxidative stress. J Toxicol Pathol 2016; 29: 247-252.

[8] Pal D, Suman S, Kolluru V, Sears S, Das TP, Alatassi H, Ankem MK, Freedman JH and Damodaran C. Inhibition of autophagy prevents cadmium-induced prostate carcinogenesis. Br J Cancer 2017; 117: 56-64.

[9] Khare D, Mitsuda N, Lee S, Song WY, Hwang D, Ohme-Takagi M, Martinoia E, Lee Y and Hwang

JU. Root avoidance of toxic metals requires the GeBP-LIKE 4 transcription factor in Arabidopsis thaliana. New Phytol 2017; 213: 1257-1273.

[10] Santana VP, Salles ES, Correa DE, Goncalves BF, Campos SG, Justulin LA, Godinho AF and Scarano WR. Long-term effects of perinatal exposure to low doses of cadmium on the prostate of adult male rats. Int J Exp Pathol 2016; 97: 310-316.

[11] Dong YX, Cao JT, Liu YM and Ma SH. A novel immunosensing platform for highly sensitive prostate specific antigen detection based on dual-quenching of photocurrent from CdSe sensitized TiO2 electrode by gold nanoparticles decorated polydopamine nanospheres. Biosens Bioelectron 2017; 91: 246-252.

[12] Augustyniak M, Plachetka-Bozek A, Kafel A, Babczynska A, Tarnawska M, Janiak A, Loba A, Dziewiecka M, Karpeta-Kaczmarek J and Zawisza-Raszka A. Phenotypic plasticity, epigenetic or genetic modifications in relation to the duration of Cd-exposure within a microevolution time range in the beet armyworm. PLoS One 2016; 11: e0167371.

[13] Kuang X, Gu JD, Tie B, Yao B and Shao J. Interactive effects of cadmium and Microcystis aeruginosa (cyanobacterium) on the growth, antioxidative responses and accumulation of cadmium and microcystins in rice seedlings. Ecotoxicology 2016; 25: 1588-1599.

[14] Liu G, Zou H, Luo T, Long M, Bian J, Liu X, Gu J, Yuan Y, Song R, Wang Y, Zhu J and Liu Z. Caspase-dependent and caspase-independent pathways are involved in cadmium-induced apoptosis in primary rat proximal tubular cell culture. PLoS One 2016; 11: e0166823.

[15] Luo T, Liu G, Long M, Yang J, Song R, Wang Y, Yuan Y, Bian J, Liu X, Gu J, Zou H and Liu Z. Treatment of cadmium-induced renal oxidative damage in rats by administration of alpha-lipoic acid. Environ Sci Pollut Res Int 2017; 24: 1832-1844.

[16] Eriksen KT, Halkjaer J, Meliker JR, McElroy JA, Sorensen M, Tjonneland A and Raaschou-Nielsen O. Dietary cadmium intake and risk of prostate cancer: a Danish prospective cohort study. BMC Cancer 2015; 15: 177.

[17] Bakshi S, Zhang X, Godoy-Tundidor S, Cheng RY, Sartor MA, Medvedovic M and Ho SM. Transcriptome analyses in normal prostate epithelial cells exposed to low-dose cadmium: oncogenic and immunomodulations involving the action of tumor necrosis factor. Environ Health Perspect 2008; 116: 769-776.

[18] Chen C, Xun P, Nishijo M, Carter S and He K. Cadmium exposure and risk of prostate cancer: a meta-analysis of cohort and case-control studies among the general and occupational populations. Sci Rep 2016; 6: 25814.

[19] Julin B, Wolk A, Johansson JE, Andersson SO, Andren O and Akesson A. Dietary cadmium exposure and prostate cancer incidence: a population-based prospective cohort study. Br J Cancer 2012; 107: 895-900.

[20] Ma T, Wang M, Gong S and Tian B. Impacts of sediment organic matter content and pH on ecotoxicity of coexposure of TiO2 nanoparticles and cadmium to freshwater snails bellamya aeruginosa. Arch Environ Contam Toxicol 2017; 72: 153-165.

[21] Satarug S, Nishijo M, Ujjin P, Vanavanitkun Y, Baker JR and Moore MR. Evidence for concurrent effects of exposure to environmental cadmium and lead on hepatic CYP2A6 phenotype and renal function biomarkers in nonsmokers. Environ Health Perspect 2004; 112: 1512-1518.

[22] Baecklund M, Pedersen NL, Bjorkman L and Vahter M. Variation in blood concentrations of cadmium and lead in the elderly. Environ Res 1999; 80: 222-230.

[23] Aimola P, Carmignani M, Volpe AR, Di Benedetto A, Claudio L, Waalkes MP, van Bokhoven A, Tokar EJ and Claudio PP. Cadmium induces p53-dependent apoptosis in human prostate epithelial cells. PLoS One 2012; 7: e33647.

[24] Aliomrani M, Sahraian MA, Shirkhanloo H, Sharifzadeh M, Khoshayand MR and Ghahremani MH. Blood concentrations of cadmium and lead in multiple sclerosis patients from Iran. Iran J Pharm Res 2016; 15: 825-833.

[25] Nemmiche S. Oxidative signaling response to cadmium exposure. Toxicol Sci 2017; 156: 4-10.

[26] Nemmiche S and Guiraud P. Cadmium-induced oxidative damages in the human BJAB cells correlate with changes in intracellular trace elements levels and zinc transporters expression. Toxicol In Vitro 2016; 37: 169-177.

[27] Pasquali F, Agrimonti C, Pagano L, Zappettini A, Villani M, Marmiroli M, White JC and Marmiroli N. Nucleo-mitochondrial interaction of yeast in response to cadmium sulfide quantum dot exposure. J Hazard Mater 2017; 324: 744-752.

[28] Song B, Du J, Feng Y, Gao YJ and Zhao JS. Co-expressed differentially expressed genes and long non-coding RNAs involved in the celecoxib treatment of gastric cancer: an RNA sequencing analysis. Exp Ther Med 2016; 12: 2455-2468.

[29] Chang J, Jung HJ, Jeong SH, Kim HK, Han J and Kwon HJ. A mutation in the mitochondrial protein UQCRB promotes angiogenesis through the generation of mitochondrial reactive oxygen species. Biochem Biophys Res Commun 2014; 455: 290-297.

[30] Mordaunt DA, Jolley A, Balasubramaniam S, Thorburn DR, Mountford HS, Compton AG,

Nicholl J, Manton N, Clark D, Bratkovic D, Friend K and Yu S. Phenotypic variation of TTC19-deficient mitochondrial complex III deficiency: a case report and literature review. Am J Med Genet A 2015; 167: 1330-1336.

[31] Oliva-Biénzobas V, Navas A, C Astiazarán M, Chacón-Camacho OF, A Bermúdez-Magner J, Takane M, Graue-Hernández E, Zenteno JC. CYP1B1 cytopathy: uncommon phenotype of a homozygous CYP1B1 deletion as internal corneal ulcer of von hippel. Cornea 2017; 36: 1256-1259.

[32] Petersson SJ, Christensen LL, Kristensen JM, Kruse R, Andersen M and Hojlund K. Effect of testosterone on markers of mitochondrial oxidative phosphorylation and lipid metabolism in muscle of aging men with subnormal bioavailable testosterone. Eur J Endocrinol 2014; 171: 77-88.

[33] Shimada T, Murayama N, Kakimoto K, Takenaka S, Lim YR, Yeom S, Kim D, Yamazaki H, Guengerich FP and Komori M. Oxidation of 1-chloropyrene by human CYP1 family and CYP2A subfamily cytochrome P450 enzymes: catalytic roles of two CYP1B1 and five CYP2A13 allelic variants. Xenobiotica 2017; 1-11.

[34] Sparks LM, Xie H, Koza RA, Mynatt R, Hulver MW, Bray GA and Smith SR. A high-fat diet coordinately downregulates genes required for mitochondrial oxidative phosphorylation in skeletal muscle. Diabetes 2005; 54: 1926-1933.

[35] Bertin G and Averbeck D. Cadmium: cellular effects, modifications of biomolecules, modulation of DNA repair and genotoxic consequences (a review). Biochimie 2006; 88: 1549-1559.

[36] Xiong X, Zhao Y, He H and Sun Y. Ribosomal protein S27-like and S27 interplay with p53-MDM2 axis as a target, a substrate and a regulator. Oncogene 2011; 30: 1798-1811.